CVI Journals.ASM.org

Therapeutic Transcutaneous Immunization with a Band-Aid Vaccine Resolves Experimental Otitis Media

Laura A. Novotny,[a] John D. Clements,[b] Lauren O. Bakaletz[a]

Center for Microbial Pathogenesis, The Research Institute at Nationwide Children's Hospital, and The Ohio State University College of Medicine, Columbus, Ohio, USA[a]; Department of Microbiology and Immunology, Tulane University School of Medicine, New Orleans, Louisiana, USA[b]

Transcutaneous immunization (TCI) is a noninvasive strategy to induce protective immune responses. We describe TCI with a band-aid vaccine placed on the postauricular skin to exploit the unique organization of the stratum corneum and to promote the development of immune responses to resolve active experimental otitis media due to nontypeable *Haemophilus influenzae* (NTHI). This therapeutic immunization strategy induced significantly earlier resolution of middle ear fluid and rapid eradication of both planktonic and mucosal biofilm-resident NTHI within 7 days after receipt of the first immunizing band-aid vaccine. Efficacy was ascribed to the homing of immunogen-bearing cutaneous dendritic cells to the nasal-associated lymphoid tissue, induction of polyfunctional $CD4^+$ T cells, and the presence of immunogen-specific IgM and IgG within the middle ear. TCI using band-aid vaccines could expand the use of traditional parenteral preventative vaccines to include treatment of active otitis media, in addition to other diseases of the respiratory tract due to NTHI.

Transcutaneous immunization (TCI) offers multiple advantages as an immunization strategy; it is noninvasive, which may aid in acceptance and compliance, and reduced costs are associated with vaccine production and administration, as delivery devices may be simplified or eliminated and trained medical personnel are not required, characteristics that could allow for vaccine distribution beyond developed countries (1, 2). TCI induces both systemic and mucosal immune responses (3–6), important features as the mucosae represent critical defensive barriers that also respond immunologically to insults (7). Thus, TCI exhibits potential as a simple efficacious method to induce protective immune responses and thereby limit disease.

One of the most common diseases of childhood is otitis media (OM). It is estimated that 709 million cases of acute OM and 65 million to 330 million episodes of chronic secretory OM occur each year worldwide (8, 9). While deaths due to OM are not common in developed countries, complications of chronic suppurative OM result in the deaths of 50,000 children <5 years of age in developing countries (10, 11). Furthermore, morbidity associated with OM is significant for all children worldwide. Nontypeable *Haemophilus influenzae* (NTHI) is the predominant pathogen in chronic OM, recurrent OM, and OM associated with treatment failure, and NTHI biofilms within the middle ear contribute significantly to pathogenesis (12, 13). Biofilms within the middle ear facilitate the chronicity and recalcitrance of OM and often require prolonged treatment with an antimicrobial. This management strategy is of concern due to the emergence of multiple antibiotic-resistant bacteria (14, 15). Thus, it is desirable develop better methods to manage OM.

Previous work demonstrated that TCI with chimV4, a novel chimeric antigen that targets the critical NTHI adhesins OMP P5 and the type IV pilus (Tfp) (16), admixed with the adjuvant LT(R192G/L211A), a double mutant of *Escherichia coli* heat-labile enterotoxin (dmLT) (17), induces significant preventative and therapeutic efficacy against experimental NTHI-induced OM when delivered by rubbing onto the skin of the outer ear (18, 19). We now consider a more practical application of TCI for humans, particularly very young children, and envision the use of a small adhesive bandage to administer vaccine formulations. Whereas cutaneous delivery systems typically rely on abrasion or surface stripping procedures to remove the stratum corneum to gain access to the dermis and epidermis (5, 20), we placed circular adhesive bandages ("band-aid vaccines") onto the intact skin of animals with active OM. Immunization was focused on the head and neck region with the intent to induce immune responses in proximity to the middle ear, because it is appreciated that there is compartmentalization of the mucosal immune system (21). The postauricular region was specifically targeted because the stratum corneum is uniquely organized in a stacked arrangement, in contrast to the more typical "brick-and-mortar" stratification found elsewhere on the body (22), which could facilitate sampling by underlying antigen-presenting cells. We contrasted the findings with those observed for immunization at the nape of the neck, a site adjacent to the postauricular region where the stratum corneum is not stacked linearly. Our data revealed that anatomical placement of the band-aid vaccine significantly influenced disease resolution and that eradication of NTHI from the middle ear began within 7 days after the first immunization. These data support the continued development of TCI using band-aid vaccines as a simple noninvasive strategy to induce therapeutic immune responses against NTHI-induced OM.

Received 13 February 2015 **Returned for modification** 9 March 2015
Accepted 14 May 2015

Accepted manuscript posted online 27 May 2015

Citation Novotny LA, Clements JD, Bakaletz LO. 2015. Therapeutic transcutaneous immunization with a band-aid vaccine resolves experimental otitis media. Clin Vaccine Immunol 22:867–874. doi:10.1128/CVI.00090-15.

Editor: H. F. Staats

Address correspondence to Lauren O. Bakaletz, lauren.bakaletz@nationwidechildrens.org.

doi:10.1128/CVI.00090-15

MATERIALS AND METHODS

Animals. Adult (500 to 950 g) chinchillas (*Chinchilla lanigera*; Rauscher's Chinchilla Ranch) without evidence of middle ear infection or serum antibody reactivity to outer membrane proteins of NTHI 86-028NP were used. The numbers of chinchillas included in each experiment were as follows: to examine the cellular organization of the stratum corneum in the postauricular region versus the nape, 3 animals; to examine whether anatomical placement of the band-aid vaccine influenced vaccine efficacy, 3 animals per cohort plus 3 chinchillas sacrificed prior to immunization to obtain baseline bacterial burden values (21 total); to track the migration of cutaneous dendritic cells after TCI, 3 chinchillas per cohort (9 total); to examine intracellular cytokine production by $CD4^+$ T cells after TCI, 3 animals per cohort (6 total); to examine the kinetics of disease resolution after TCI in the postauricular region, 4 animals per cohort for each time point plus 4 animals sacrificed prior to immunization to obtain baseline bacterial burden values (28 total). Animal studies were performed under a protocol approved by The Research Institute at Nationwide Children's Hospital Institutional Animal Care and Use Committee.

Bacterial isolate. NTHI 86-028NP is a minimally passaged clinical isolate that was collected from the nasopharynx of a child with chronic OM; it has been characterized extensively (23, 24).

Vaccine formulations. ChimV4 is a recombinant chimeric protein designed to target two critical NTHI adhesins, i.e., OMP P5 and the type IV pilus (Tfp), by utilizing a recombinant, soluble, N-terminally truncated form of PilA, the majority subunit of NTHI Tfp, as both an immunogen and carrier for a 24-mer B-cell epitope identified within NTHI OMP P5 (16). Formulations contained 10 μg chimV4 admixed with 10 μg LT(R192G/L211A), a double mutant of *E. coli* heat-labile enterotoxin (dmLT) as the adjuvant (17), 10 μg dmLT alone, or an equivalent volume of pyrogen-free saline solution.

Challenge and immunization. All chinchillas were first challenged transbullarly with 1,000 CFU NTHI strain 86-028NP per bulla, to induce experimental OM. At that time, the fur directly caudal to each pinna (postauricular region) or at the nape of the neck was plucked, to permit resolution of any nonspecific inflammation induced by hair removal prior to immunization. Four days later, when middle ear biofilms are well established and clinically relevant signs of OM are observed (19, 25, 26), animals were immunized by placement of a circular adhesive bandage (CVS Pharmacy brand) in each postauricular region (two band-aid vaccines were applied, and the total formulation dosage was divided equally between the bandages) or at the nape of the chinchilla neck (one band-aid was applied). All band-aid vaccines were removed after 24 h. Animals received band-aid vaccine boosters 7 days later.

Video otoscopy. Video otoscopy using a 3-inch, 0° probe connected to a digital camera system (MedRx, Largo, FL) was utilized to monitor signs of tympanic membrane inflammation and/or the presence of fluid within the middle ear space. Overall signs of OM were blindly rated on a scale of 0 to 4, and middle ears with scores of ≥2.0 were considered positive for OM, as middle ear fluid (MEF) was visible behind the tympanic membrane (27). According to established protocol, each middle ear was considered independently (18, 19, 26, 28–30), and the percentage of middle ears with OM was calculated for each cohort.

Collection and assessment of middle ear fluid samples. Upon sacrifice, bullae were dissected and MEF was collected. The adherent middle ear mucosal biofilms were also collected and individually homogenized in sterile saline solution. It is well established in chinchilla models of OM that each middle ear should be considered independently (18, 19, 25, 26, 31–40); therefore, MEF and biofilm homogenates collected from the left and right middle ears were individually plated on chocolate agar to semiquantitatively assess the relative numbers of NTHI in the planktonic and adherent populations. MEF samples were then clarified by centrifugation, and supernatants were stored at −80°C until determination of immunoglobulin profiles as described below.

Visualization of stratum corneum cellular architecture. Skin samples from the chinchilla postauricular region and the nape of the neck were harvested from 3 chinchillas and snap-frozen in Tissue-Tek O.C.T. Compound (Sakura Fintek, Torrance, CA). To visualize the orientation of corneocytes within the stratum corneum, 3 drops of 0.4 N sodium hydroxide plus 2 drops of 0.1% methylene blue were applied to 5-μm-thick sections of frozen skin, and the specimens were incubated for 5 min at room temperature to allow the corneocytes to swell (41).

Tracking of migration of cutaneous dendritic cells. The immunogen chimV4 and the adjuvant dmLT were separately labeled with DyLight 650 NHS Ester (Pierce Biotechnology, Rockford, IL) according to the manufacturer's instructions. Labeled chimV4 admixed with unlabeled dmLT or labeled dmLT alone was applied to band-aids, which were then affixed to the skin in the postauricular region or at the nape of the neck of three chinchillas for each formulation, as described. After 24 h, the nasal-associated lymphoid tissue (NALT) and cervical, axillary, and parotid lymph nodes were collected and processed to yield single-cell suspensions. Spleens were homogenized in Hanks' balanced salt solution (HBSS) (Mediatech Corning, Manassas, VA) using GentleMACs C-tubes (Miltenyi Biotec GmbH, Bergisch Gladbach, Germany), the homogenates were centrifuged through Ficoll-Paque PLUS (GE Healthcare, Pittsburgh, PA), and cells at the interface were collected. To control for nonspecific activation of cutaneous dendritic cells, lymphoid tissues were also collected from three animals that had received adhesive bandages in which the gauze pads had been hydrated with pyrogen-free saline solution. Cell suspensions were stained with fluorescein isothiocyanate (FITC)-conjugated goat anti-rat CD11c (AbD Serotec, Kidlington, United Kingdom), and 50,000 events were collected with a BD Accuri C6 cytometer (BD Biosciences, San Jose, CA). The presence of DyLight 650-positive signals within the $CD11c^+$ population was identified using FlowJo software (TreeStar, Inc., Ashland, OR).

Intracellular cytokine detection. Upon sacrifice, the NALT, the cervical, axillary, and parotid lymph nodes, and the spleen were collected in phenol red-free RPMI 1640 medium (Mediatech Corning) with 0.5% fetal bovine serum (FBS) (GE Healthcare HyClone) and were prepared as described above. At least 10^5 cells per lymphoid tissue were activated in the presence of BD GolgiStop inhibitor and subsequently were stained using the BD human Th1/Th2/Th17 phenotyping kit (BD Biosciences). A total of 20,000 events were analyzed by flow cytometry, and the production of interleukin 17A (IL-17A) and gamma interferon (IFN-γ) within the $CD4^+$ population was determined with FlowJo software. Three animals per cohort were screened; because chinchillas are outbred animals, lymphoid cells were processed and assayed for individual animals.

Enumeration of chimV4-specific antibody-secreting cells via enzyme-linked immunospot assay. To enumerate antibody-secreting cells (ASCs) in bone marrow, wells of 96-well filtration plates were coated with 5 μg chimV4 overnight at 4°C and then were blocked with phenol red-free RPMI 1640 medium plus 10% heat-inactivated FBS. Cells isolated from femur bone marrow (42) were activated for 5 days with resiquimod (Sigma-Aldrich, St. Louis, MO) at 1 μg/ml and recombinant human IL-2 (R&D Systems, Inc., Minneapolis, MN) at 10 ng/ml, seeded at densities of 5×10^4, 1×10^5, and 5×10^5 cells per well in triplicate, and incubated for 5 h at 37°C in 5% CO_2. Because chinchillas are outbred, cells were processed and assessed for individual animals. Goat anti-rat IgM, IgA, or IgG conjugated to horseradish peroxidase (HRP) (Bethyl Laboratories, Montgomery, TX) was applied, and spots were developed using a 3,3′-diaminobenzidine (DAB) peroxidase substrate kit (Vector Laboratories, Burlingame, CA). Spots were detected and enumerated using an EliScan+ system (A.EL.VIS GmbH, Hannover, Germany).

Quantitation of chimV4-specific immunoglobulins. To quantitate chimV4-specific antibody isotypes within MEF, a slot blot assay was performed. Immun-Blot LF polyvinylidene difluoride (PVDF) membranes (Bio-Rad, Hercules, CA) were prepared by sequential washes in methanol, cold Towbin buffer (25 mM Tris, 192 mM glycine, 20% methanol [pH 8.3]), and distilled water prior to coating with 1 μg chimV4 per slot by vacuum aspiration. Membranes were incubated with clarified MEF and immunogen-specific antibodies were revealed with goat anti-rat IgM,

IgA, or IgG conjugated to FITC (Bethyl Laboratories). A standard curve was generated by coating membranes with purified rat-specific IgM, IgA, and IgG followed by incubation with rat reference serum. Dry membranes were imaged with a FluoroChem M system (ProteinSimple, San Jose, CA), and the fluorescent intensity of each band was determined with AlphaView SA software (ProteinSimple).

Statistics. Statistical significance was calculated using GraphPad Prism software (GraphPad Software, Inc., La Jolla, CA). Statistical differences among bacterial counts in MEF and mucosal biofilms were determined using Kruskal-Wallis one-way analysis of variance (ANOVA) and Dunn's method for multiple comparisons. Significant differences in percentages of middle ears with OM were assessed with the Mantel-Cox log-rank test, with an event being classified as resolution of OM. Differences in numbers of ASCs and antibody titers were determined by one-way ANOVA with Tukey's multiple-comparison test. For all analyses, P values of ≤ 0.05 were considered significant.

RESULTS

Cellular organization of stratum corneum in postauricular region versus nape. The stratum corneum represents a formidable barrier to skin vaccination strategies. Because the cellular organization of the chinchilla stratum corneum in either the nape of the neck or the postauricular region has not been reported, and to understand any differences in efficacy related to anatomical placement of the band-aid vaccines, skin specimens from these sites were collected and the organization of the cells within the stratum corneum was examined by microscopy. The corneocytes in the postauricular region were linearly aligned (Fig. 1A), whereas a classic brick-and-mortar arrangement was observed at the nape (Fig. 1B) (22, 41). We thus hypothesized that the unique alignment of cells in the postauricular region would likely allow for easier sampling of topically placed immunogens by cutaneous antigen-presenting cells.

Anatomical placement of band-aid vaccines influences resolution of experimental otitis media. With the goal of developing a means to administer vaccine formulations noninvasively without alteration of the skin surface, we utilized a regular small circular adhesive bandage (Fig. 2A). Each middle ear was individually assessed for the relative quantities of NTHI within MEF and mucosal biofilms, as is standard for this experimental model (18, 19, 25, 26, 31–39). Four days after middle ear challenge with NTHI, all middle ears exhibited robust experimental OM, with high concentrations of NTHI within both MEF and mucosal biofilms (Fig. 2B and C). Band-aid vaccines were then applied to the skin either in the postauricular region or at the nape of the neck. One week after receipt of the second dose of chimV4 plus dmLT at the nape, a 2-log-unit reduction in NTHI levels was detected in MEF samples, compared to receipt of saline or the adjuvant dmLT ($P \leq 0.05$) (Fig. 2B). Moreover, 50% of MEF samples were culture negative after the receipt of chimV4 plus dmLT at the nape, whereas 100% of MEF samples were culture positive after the receipt of saline or dmLT. Immunization with chimV4 plus dmLT in the postauricular region resulted in 3- and 2-log-unit lower NTHI levels in MEF, compared to saline and dmLT, respectively ($P \leq 0.01$ and $P \leq 0.05$, respectively). Also, 67% of MEF samples were culture negative after receipt of chimV4 plus dmLT in the postauricular region, whereas 100% and 67% of MEF samples were culture positive in the cohorts treated with saline and dmLT, respectively.

Within mucosal biofilms, a 2-log-unit reduction in NTHI levels resulted from TCI at the nape with chimV4 plus dmLT, compared to receipt of saline ($P \leq 0.01$), with a 1-log-unit reduction in comparison with dmLT (Fig. 2C). Administration of chimV4 plus dmLT in the postauricular region resulted in 3- and 1-log-unit lower NTHI levels in mucosal biofilms, compared to saline and dmLT, respectively ($P \leq 0.01$ and $P \leq 0.05$, respectively). Among cohorts treated with chimV4 plus dmLT, immunization in the postauricular region resulted in greater percentages of culture-negative MEF samples (67%) and mucosal biofilms (33%), compared to TCI at the nape (50% and 0%, respectively). Moreover, TCI with chimV4 plus dmLT in the postauricular region resulted in a 1.3-log-unit reduction in NTHI levels, compared to treatment at the nape ($P \leq 0.01$). Thus, TCI using band-aid vaccines to administer chimV4 plus dmLT resolved active NTHI-induced OM; furthermore, induction of bacterial clearance was superior after TCI in the postauricular region, compared to the nape.

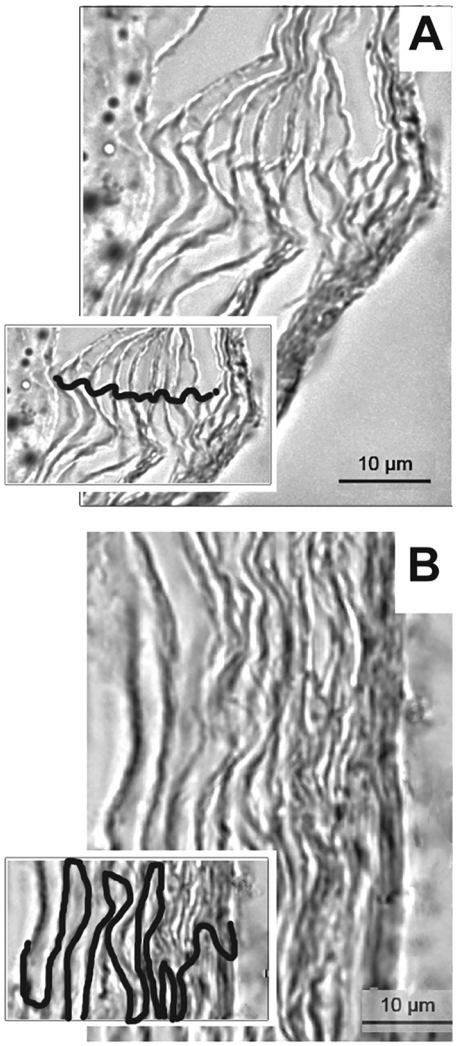

FIG 1 Organization of corneocytes of the stratum corneum from skin samples collected from the chinchilla postauricular region (A) and the nape (B), as shown by microscopy. Insets, visualization of corneocyte stratification with cellular junctions traced. Scale bars, 10 μm.

Migration of cutaneous dendritic cells after TCI. To track the migration of cutaneous dendritic cells after uptake of immunogen and to reveal sites of immune induction, fluorescent DyLight 650-

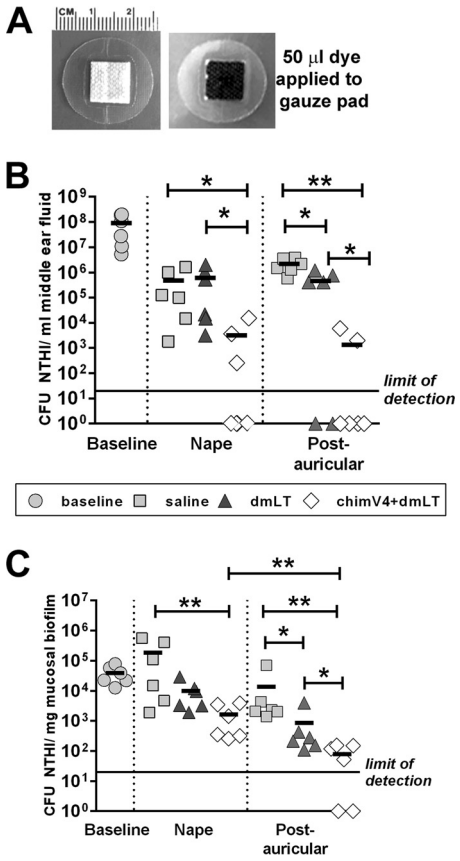

FIG 2 Induction of significantly more rapid eradication of NTHI from both middle ear fluid samples and mucosal biofilms by TCI with chimV4 plus dmLT by a band-aid vaccine placed in the postauricular region. (A) Circular adhesive bandage utilized in these studies, demonstrating retention of a 50-μl fluid volume on the gauze pad. (B and C) CFU of NTHI per milliliter of middle ear fluid (B) and CFU of NTHI per milligram of mucosal biofilm (C) collected prior to immunization (baseline) and 7 days after receipt of the second weekly band-aid vaccine (nape and postauricular region) for each cohort. Significant reductions in NTHI levels were detected after receipt of chimV4 plus dmLT, and TCI in the postauricular region was superior to placement at the nape in resolving experimental OM. Values for individual middle ears are plotted, and the mean for each cohort is indicated by short horizontal lines. *, $P \leq 0.05$; **, $P \leq 0.01$, one-way ANOVA.

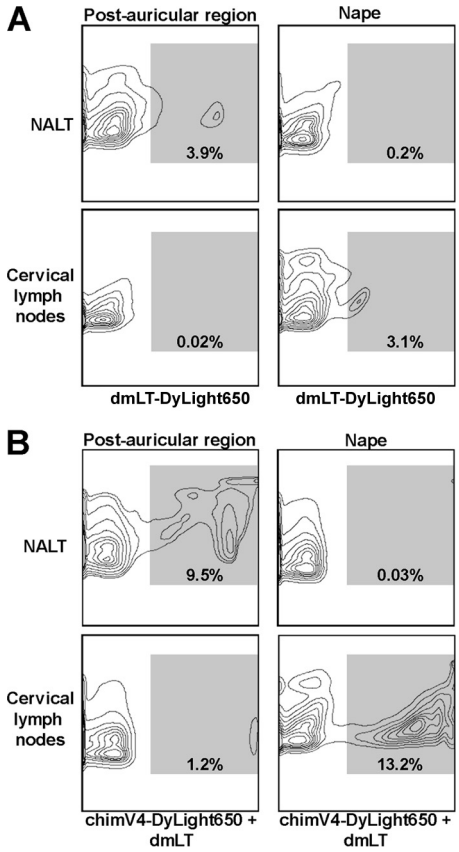

FIG 3 Directional migration of CD11c$^+$ cells after TCI. Representative flow cytometry contour plots depict dmLT- and chimV4-specific signals within CD11c$^+$ cells isolated from the NALT and cervical lymph nodes after TCI in the postauricular region and nape with fluorescently labeled dmLT (A) and fluorescently labeled chimV4 admixed with unlabeled dmLT (B). dmLT$^+$ and chimV4$^+$ fluorescent signals (indicated by the shaded region within each plot and quantitated as the percentage of CD11c$^+$ cells) were detected within the NALT after immunization in the postauricular region and within the cervical lymph nodes after immunization at the nape; therefore, the anatomical site of band-aid vaccine placement influenced the migration of cutaneous antigen-presenting cells. Moreover, mixing chimV4 with dmLT resulted in enhanced migration.

labeled chimV4 was admixed with unlabeled dmLT and utilized for immunization of three chinchillas. Lymphoid tissues were collected 24 h later and assessed for DyLight 650-specific fluorescence within CD11c$^+$ cells. To identify the contribution of dmLT to the activation of cutaneous CD11c$^+$ cells, fluorescently labeled dmLT was administered by band-aid vaccine to a separate cohort of animals. dmLT-specific fluorescent signals were detected only within the NALT and cervical lymph nodes; therefore, only results obtained from these lymphoid tissues are shown. After immunization in the postauricular region, 3.9% of CD11c$^+$ cells isolated from the NALT showed positive fluorescent signals for dmLT (Fig. 3A). Immunization at the nape, however, induced migration of dmLT-bearing CD11c$^+$ cells to the cervical lymph nodes. Collectively, these data indicated a migration pattern that was influenced by the anatomical site to which the band-aid vaccines were applied.

This observation was enhanced by mixing fluorescently labeled chimV4 with unlabeled dmLT. TCI with chimV4 in the postauricular region resulted in migration of immunogen-bearing CD11c$^+$ cells exclusively to the NALT and not the cervical lymph nodes (Fig. 3B). In contrast, immunization at the nape induced migration to the cervical lymph nodes but not the NALT (Fig. 3B). Of the CD11c$^+$ cells collected from the NALT after TCI in the postauricular region, 9.5% were chimV4$^+$, whereas 1.2% in the cervical lymph nodes were positive. After TCI at the nape, 0.03% of CD11c$^+$ cells in the NALT were also chimV4$^+$; however, 13.2% in the cervical lymph nodes were positive. These data demonstrated that band-aid vaccine placement in the postauricular region or at the nape had direct effects on the relative migration of antigen-presenting cells to the NALT or cervical lymph nodes, respectively.

TCI in postauricular region or nape results in different sites of immune induction. We next examined cytokine production by CD4$^+$ T cells within the NALT and cervical lymph nodes. As anticipated based on data presented in Fig. 3, CD4$^+$ T cells producing IFN-γ and IL-17A were detected exclusively within the NALT

TABLE 1 Fold increases in IFN-γ- and IL-17A-specific mean fluorescent intensities within $CD4^+$ T cells collected from NALT and cervical lymph nodes of animals immunized with dmLT or chimV4 plus dmLT versus saline

	Fold increase in specific fluorescence intensity (mean ± SEM)							
	Immunization in postauricular region				Immunization at nape			
	dmLT		chimV4 + dmLT		dmLT		chimV4 + dmLT	
Sample	IFN-γ	IL-17A	IFN-γ	IL-17A	IFN-γ	IL-17A	IFN-γ	IL-17A
NALT	1.1 ± 0.2	1.2 ± 0.3	2.1 ± 0.3	1.9 ± 0.4	1.0 ± 0	1.0 ± 0	1.0 ± 0	1.0 ± 0
Cervical lymph nodes	1.0 ± 0	1.0 ± 0	1.0 ± 0.1	1.0 ± 0	1.1 ± 0.3	1.1 ± 0.2	1.5 ± 0.3	1.3 ± 0.2

of animals immunized in the postauricular region (Table 1), whereas activated cells were identified within the cervical lymph nodes after immunization at the nape. Compared to animals that received band-aid vaccines hydrated with saline, a 2.1-fold increase in mean fluorescence specific for IFN-γ and a 1.9-fold increase in that for IL-17A were detected within the NALT of animals immunized with chimV4 plus dmLT in the postauricular region; alternatively, 1.5- and 1.3-fold increases in mean fluorescence, respectively, were detected within the cervical lymph nodes after TCI at the nape with chimV4 plus dmLT, compared to saline. These data revealed that band-aid vaccine placement in the postauricular region or at the nape resulted in different sites of immune activation, which is a critical observation for understanding the superiority of efficacy achieved with immunization at a postauricular site, as shown in Fig. 2. Moreover, the production of IFN-γ and IL-17A, utilized herein as indicators of Th1- and Th17-type immune responses, respectively, indicated that polyfunctional immune responses were induced by TCI with chimV4 plus dmLT, corroborating previous data obtained with this immunogen and adjuvant (19).

Kinetics of disease resolution. In an expanded study, we next examined the kinetics of disease resolution after immunization in the postauricular region, the site that induced superior eradication of NTHI from the middle ear (Fig. 2). As a clinically relevant assessment for the resolution of OM, the tympanic membranes of each animal were visualized by video otoscopy, to discern signs of inflammation and the presence of MEF. Prior to immunization, MEF was observed in 100% of middle ears, as expected due to direct challenge of the middle ears of all animals with NTHI 4 days earlier (Fig. 4A). MEF persisted in all middle ears (8/8 ears) in the cohort that received saline for the duration of the study. In the cohort treated with dmLT, 88% of middle ears (7/8 ears) were positive for the presence of middle ear fluid, which decreased to 75% of middle ears (6/8 ears) 7 days after TCI. However, 7 days after receipt of the first dose of chimV4 plus dmLT, MEF was observed in only 63% of middle ears (5/8 ears), which was further reduced to 13% (1/8 ears) after receipt of the second band-aid vaccine. These data demonstrated that TCI with chimV4 plus dmLT induced rapid resolution of OM (MEF), which was significant, compared to receipt of dmLT or saline ($P \leq 0.05$ versus dmLT; $P \leq 0.001$ versus saline).

We next examined the ability of TCI to induce immune responses that eradicated NTHI from both the planktonic population and mucosal biofilms established within the middle ear. Receipt of dmLT promoted significant but nonspecific reductions in CFU of NTHI in MEF, compared to saline, at each time point ($P \leq 0.01$) (Fig. 4B), a result we previously reported following use of this powerful adjuvant in outbred, nonspecific-pathogen-free

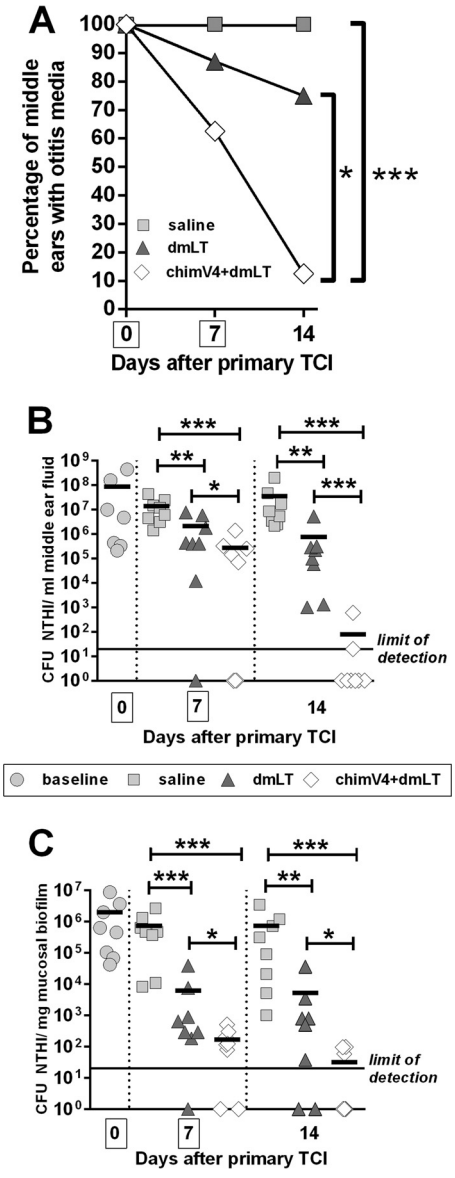

FIG 4 Kinetics of resolution of experimental OM after TCI with band-aid vaccines placed in the postauricular region. (A) Percentages of middle ears with OM after TCI, as determined by video otoscopy. The mean ± standard error of the mean (SEM) for each cohort is shown. *, $P \leq 0.05$; ***, $P \leq 0.001$, Mantel-Cox log-rank test. (B) CFU of NTHI per milliliter of middle ear fluid. (C) CFU of NTHI per milligram of mucosal biofilm. TCI with chimV4 plus dmLT eradicated NTHI from middle ear fluid samples and mucosal biofilms beginning 7 days after receipt of the first band-aid vaccine. Boxes around days 0 and 7 on the *x* axes indicate days of immunization. Values for individual middle ears are plotted, and the mean for each cohort is indicated by short horizontal lines. *, $P \leq 0.05$; **, $P \leq 0.01$; ***, $P \leq 0.001$, one-way ANOVA.

chinchillas (18, 19). TCI with chimV4 admixed with dmLT to focus the immune responses on NTHI induced a 1-log-unit reduction after receipt of one band-aid vaccine versus dmLT ($P \leq 0.05$) and a 2-log-unit reduction versus saline ($P \leq 0.001$). This response was boosted by administration of a second band-aid vaccine 1 week later, as a 4-log-unit reduction in NTHI was shown versus dmLT ($P \leq 0.001$) and a 6-log-unit reduction versus saline ($P \leq 0.001$). After receipt of the second dose of chimV4 plus dmLT, <80 CFU of NTHI remained within 25% of ears in this cohort, with the remaining 75% of middle ear fluid samples being culture negative for NTHI.

Within NTHI biofilms that were adherent to the middle ear mucosa, delivery of saline by band-aid vaccine induced no reduction in bacterial concentrations (Fig. 4C). Seven days after administration of dmLT, however, a significant 2-log-unit reduction in NTHI, compared to saline ($P \leq 0.001$), was observed in the ears that still contained mucosal biofilms, although no significant further decrease in bacterial concentrations was achieved with receipt of a second dose of adjuvant only. In contrast, chimV4 admixed with dmLT induced significant 0.5- and 2-log-unit reductions in NTHI, compared to dmLT ($P \leq 0.05$), in the ears that still contained mucosal biofilms on days 7 and 14, respectively. Moreover, mucosal biofilms were eradicated from 25% of the middle ears after delivery of the first immunizing band-aid vaccine with chimV4 plus dmLT, and administration of a second dose induced eradication of mucosal biofilms from 63% of the middle ears. Collectively, this kinetic study demonstrated that TCI with a band-aid vaccine containing chimV4 plus dmLT induced rapid immune responses, beginning at least 7 days after receipt of the first dose.

Assessment of chimV4-specific antibodies. Induction of serum antibodies has long been considered a correlate of immune protection for OM following natural disease (43). However, TCI does not induce a robust serum antibody response (18, 19). Therefore, here we determined the relative quantities of chimV4-specific antibody-secreting cells (ASCs) in bone marrow and the levels of immunogen-specific antibodies in MEF samples after receipt of both immunizing doses. TCI with chimV4 plus dmLT resulted in significantly greater numbers of cells that produced chimV4-specific antibodies of the IgM isotype, compared to IgG and IgA ($P \leq 0.001$ versus IgA and $P \leq 0.01$ versus IgG) (Fig. 5A). Moreover, at the site of infection within the middle ear, the relative quantities of chimV4-specific IgM in MEF samples were significantly greater than those of the IgG and IgA isotypes ($P \leq 0.001$ versus IgA and $P \leq 0.01$ versus IgG); chimV4-specific IgG was the next most abundant ($P < 0.01$ versus IgA) (Fig. 5B). While the greater concentrations of IgM-secreting ASCs and IgM in MEF samples indicated an immune response early in development, the presence of IgA- and IgG-secreting ASCs and immunoglobulin revealed that this response was maturing. Immunogen-specific antibodies were observed to be critical components mediating the clearance of NTHI from both MEF and mucosal biofilms. Collectively, these data showed that TCI induced the production of immunogen-specific ASCs and antibodies, key contributors to the eradication of NTHI and the resolution of experimental OM.

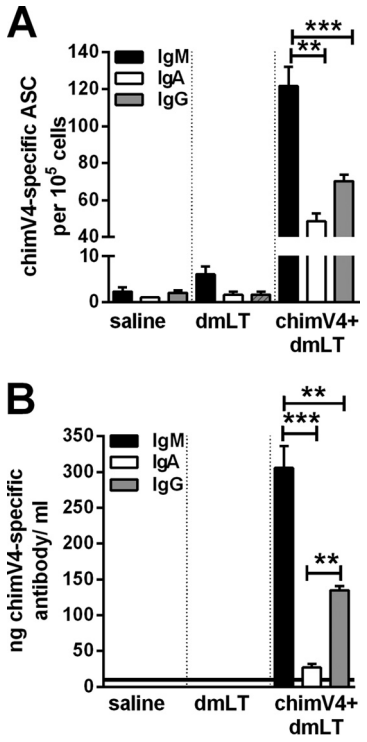

FIG 5 Quantitation of chimV4-specific antibody-secreting cells isolated from bone marrow with an enzyme-linked immunospot assay (ELISPOT) (A) and chimV4-specific antibodies in middle ear fluid samples by quantitative slot blot analysis (B) after TCI with a band-aid vaccine placed in the postauricular region. TCI induced the production of immunogen-specific ASCs and antibodies, primarily of the IgM and IgG isotypes. The horizontal line in panel B indicates the limit of detection. Means ± SEMs are shown. **, $P \leq 0.01$; ***, $P \leq 0.001$, one-way ANOVA.

DISCUSSION

We previously showed that application of NTHI adhesin-targeted immunogens, in a droplet, directly onto intact skin of the chinchilla outer ear induced eradication of NTHI from the middle ear, and we showed the utility of preventative and therapeutic TCI strategies against OM due to NTHI (18). Our current work extended these findings with the goal of developing a more practical and precise means by which to administer vaccine formulations noninvasively (ultimately to children). The skin is the largest immunocompetent organ; however, access to immune cells in the dermis and epidermis is restricted by the stratum corneum. Multiple cutaneous delivery devices are under investigation, including microneedles, abrasive skin preparation devices, jet injectors, and electroporators, all of which deliver antigen below the stratum corneum and therefore represent intradermal immunization approaches. These devices present challenges when targeting newborns and young children, due to their abrasive or invasive nature. To overcome this potential obstacle, we utilized simple circular adhesive bandages to administer a vaccine formulation on intact unmodified skin, with the goal of facilitating antigen uptake through the stratum corneum in the postauricular region (i.e., a purely transcutaneous immunization approach). To our knowledge, these data are the first to demonstrate significant therapeutic efficacy against an active bacterial disease in which robust biofilms are integral to the disease course through delivery of an immunogen onto intact skin via placement of a band-aid vaccine.

OM is a disease of the respiratory mucosa; therefore, to promote the development of mucosal immune responses in the uppermost airway, it is rational to propose vaccine application in the head and neck region, particularly because it is appreciated that

there is compartmentalization of the mucosal immune system (21). We focused on the postauricular region as an easily accessible potential site for vaccine delivery via TCI, with the knowledge that in humans the cells within the stratum corneum of the postauricular region are uniquely organized vertically, as opposed to the brick-and-mortar organization present in the rest of the body, such as the nape of the neck (41). We first confirmed that this unique arrangement of cells in the postauricular region was similar in chinchillas and, based on the enhanced resolution of experimental OM achieved with TCI in the postauricular region, in contrast to the nape, proposed that the cellular organization of the stratum corneum is important to enable vaccine antigen uptake by underlying cutaneous dendritic cells.

TCI yields robust immune responses near the site of administration, facilitated by homing of activated immune cells to nearby lymphoid tissues (21, 44, 45). Tracking the migration of cutaneous dendritic cells to lymphoid tissues after TCI in the postauricular region revealed that these immune-modulating cells homed to the NALT, whereas TCI at the nape resulted in migration to the cervical lymph nodes. We also showed that polyfunctional $CD4^+$ T cells were present within the NALT after immunization in the postauricular region, whereas immunization at the nape resulted in activated $CD4^+$ T cells within the cervical lymph nodes. Because immune induction at the NALT, a lymphoid aggregate near the site of disease within the middle ear, was significantly efficacious in resolving active NTHI-induced OM, these data revealed that anatomical placement of the band-aid vaccine was a critical consideration in the development of this cutaneous immunization strategy, as we detected regionalized immune responses that subsequently affected vaccine-induced resolution of disease. Further development of this model will utilize TCI in the postauricular region as a means to promote local protective immune responses.

In previous work, TCI through rubbing of chimV4 plus dmLT onto the pinnae, or outer ears, of chinchillas induced eradication of NTHI from the middle ears (18, 19). In the current study, elimination of NTHI was not as complete, as two of eight middle ear fluid samples and four of eight mucosal biofilms remained positive for the presence of NTHI, albeit at levels close to the limit of detection and at concentrations determined to be statistically significantly less than negative-control cohorts. The difference between the two studies may be explained by the relative accessibility of vaccine antigen applied to the gauze pad on the adhesive bandage. TCI through pipetting of the vaccine formulation directly onto the pinnae provides the opportunity for the entire dose to come into contact with cutaneous antigen-presenting cells once the vaccine is spread over the surface of the skin by rubbing, as by design. We do not yet know how fully accessible vaccine antigen that has been applied as a band-aid vaccine is, but we surmised that perhaps the full dose was not as readily available to cutaneous antigen-presenting cells when applied to the highly absorbent gauze pad. Future work will aim to answer this question and continue to optimize this efficacious delivery strategy.

Administration of dmLT alone by band-aid vaccine resulted in significant reductions in the CFU of NTHI in middle ear fluid samples and mucosal biofilms, compared to receipt of saline. This result was not unexpected, as chinchillas are outbred animals and therefore use of a potent adjuvant serves to boost nonspecific immune responses against their own flora, including Gram-negative bacteria that possess outer membrane proteins with enough similarity to proteins expressed by NTHI to result in reductions in bacterial concentrations (18, 19). This outcome was significantly enhanced by directed immunization with chimV4 that had been admixed with dmLT as the vaccine formulation, thereby focusing the baseline immune response elicited by dmLT toward the critical NTHI adhesins OMP P5 and the type IV pilus, which promoted rapid clearance of NTHI from the middle ear.

Collectively, these data demonstrated that TCI with a band-aid vaccine to deliver chimV4 plus dmLT was highly efficacious in rapidly resolving active experimental OM. The continued development of this noninvasive and nonabrasive strategy holds great promise to enable widespread distribution and to promote compliance in both developed and developing countries.

ACKNOWLEDGMENTS

We thank Jennifer Neelans for manuscript preparation, Joseph A. Jurcisek, Michael O. Ward, Jr., and Dana J. Staffen for technical assistance, and Elizabeth Norton (Tulane University) for the slot blot protocol. We also thank the Animal Resources Core at The Research Institute at Nationwide Children's Hospital for animal care and husbandry.

This work was supported by NIDCD/NIH grant R01 DC003915 to L.O.B. and NIH National Center for Advancing Translational Sciences grant 8UL1TR000090-05 to J.D.C. and L.O.B.

We report no conflicts of interest.

REFERENCES

1. **Giudice EL, Campbell JD.** 2006. Needle-free vaccine delivery. Adv Drug Deliv Rev **58:**68–89. http://dx.doi.org/10.1016/j.addr.2005.12.003.
2. **Warger T, Schild H, Rechtsteiner G.** 2007. Initiation of adaptive immune responses by transcutaneous immunization. Immunol Lett **109:**13–20. http://dx.doi.org/10.1016/j.imlet.2007.01.007.
3. **Mishra D, Mishra PK, Dubey V, Nahar M, Dabadghao S, Jain NK.** 2008. Systemic and mucosal immune response induced by transcutaneous immunization using hepatitis B surface antigen-loaded modified liposomes. Eur J Pharm Sci **33:**424–433. http://dx.doi.org/10.1016/j.ejps.2008.01.015.
4. **Lawson LB, Clements JD, Freytag LC.** 2012. Mucosal immune responses induced by transcutaneous vaccines. Curr Top Microbiol Immunol **354:**19–37.
5. **Glenn GM, Scharton-Kersten T, Alving CR.** 1999. Advances in vaccine delivery: transcutaneous immunisation. Expert Opin Investig Drugs **8:**797–805. http://dx.doi.org/10.1517/13543784.8.6.797.
6. **Frech SA, Dupont HL, Bourgeois AL, McKenzie R, Belkind-Gerson J, Figueroa JF, Okhuysen PC, Guerrero NH, Martinez-Sandoval FG, Melendez-Romero JH, Jiang ZD, Asturias EJ, Halpern J, Torres OR, Hoffman AS, Villar CP, Kassem RN, Flyer DC, Andersen BH, Kazempour K, Breisch SA, Glenn GM.** 2008. Use of a patch containing heat-labile toxin from *Escherichia coli* against travellers' diarrhoea: a phase II, randomised, double-blind, placebo-controlled field trial. Lancet **371:**2019–2025. http://dx.doi.org/10.1016/S0140-6736(08)60839-9.
7. **Russell MW, Ogra PL.** 2010. Mucosal decisions: tolerance and responsiveness at mucosal surfaces. Immunol Invest **39:**297–302. http://dx.doi.org/10.3109/08820131003729927.
8. **Monasta L, Ronfani L, Marchetti F, Montico M, Vecchi Brumatti L, Bavcar A, Grasso D, Barbiero C, Tamburlini G.** 2012. Burden of disease caused by otitis media: systematic review and global estimates. PLoS One **7:**e36226. http://dx.doi.org/10.1371/journal.pone.0036226.
9. **American Academy of Pediatrics, Subcommittee on Management of Acute Otitis Media.** 2004. Diagnosis and management of acute otitis media. Pediatrics **113:**1451–1465. http://dx.doi.org/10.1542/peds.113.5.1451.
10. **Gould JM, Matz PS.** 2010. Otitis media. Pediatr Rev **31:**102–116. http://dx.doi.org/10.1542/pir.31-3-102.
11. **Vergison A, Dagan R, Arguedas A, Bonhoeffer J, Cohen R, Dhooge I, Hoberman A, Liese J, Marchisio P, Palmu AA, Ray GT, Sanders EA, Simoes EA, Uhari M, van Eldere J, Pelton SI.** 2010. Otitis media and its consequences: beyond the earache. Lancet Infect Dis **10:**195–203. http://dx.doi.org/10.1016/S1473-3099(10)70012-8.

12. **Post JC.** 2001. Direct evidence of bacterial biofilms in otitis media. Laryngoscope **111:**2083–2094. http://dx.doi.org/10.1097/00005537-200112000-00001.
13. **Swords WE.** 2012. Nontypeable *Haemophilus influenzae* biofilms: role in chronic airway infections. Front Cell Infect Microbiol **2:**97.
14. **Song JH, Dagan R, Klugman KP, Fritzell B.** 2012. The relationship between pneumococcal serotypes and antibiotic resistance. Vaccine **30:**2728–2737. http://dx.doi.org/10.1016/j.vaccine.2012.01.091.
15. **Leibovitz E, Broides A, Greenberg D, Newman N.** 2010. Current management of pediatric acute otitis media. Expert Rev Anti Infect Ther **8:**151–161. http://dx.doi.org/10.1586/eri.09.112.
16. **Novotny LA, Adams LD, Kang DR, Wiet GJ, Cai X, Sethi S, Murphy TF, Bakaletz LO.** 2009. Epitope mapping immunodominant regions of the PilA protein of nontypeable *Haemophilus influenzae* (NTHI) to facilitate the design of two novel chimeric vaccine candidates. Vaccine **28:**279–289. http://dx.doi.org/10.1016/j.vaccine.2009.08.017.
17. **Norton EB, Lawson LB, Freytag LC, Clements JD.** 2011. Characterization of a mutant *Escherichia coli* heat-labile toxin, LT(R192G/L211A), as a safe and effective oral adjuvant. Clin Vaccine Immunol **18:**546–551. http://dx.doi.org/10.1128/CVI.00538-10.
18. **Novotny LA, Clements JD, Bakaletz LO.** 2011. Transcutaneous immunization as preventative and therapeutic regimens to protect against experimental otitis media due to nontypeable *Haemophilus influenzae*. Mucosal Immunol **4:**456–467. http://dx.doi.org/10.1038/mi.2011.6.
19. **Novotny LA, Clements JD, Bakaletz LO.** 2013. Kinetic analysis and evaluation of the mechanisms involved in the resolution of experimental nontypeable *Haemophilus influenzae*-induced otitis media after transcutaneous immunization. Vaccine **31:**3417–3426. http://dx.doi.org/10.1016/j.vaccine.2012.10.033.
20. **McKenzie R, Bourgeois AL, Frech SA, Flyer DC, Bloom A, Kazempour K, Glenn GM.** 2007. Transcutaneous immunization with the heat-labile toxin (LT) of enterotoxigenic *Escherichia coli* (ETEC): protective efficacy in a double-blind, placebo-controlled challenge study. Vaccine **25:**3684–3691. http://dx.doi.org/10.1016/j.vaccine.2007.01.043.
21. **Czerkinsky C, Holmgren J.** 2012. Mucosal delivery routes for optimal immunization: targeting immunity to the right tissues. Curr Top Microbiol Immunol **354:**1–18.
22. **Christophers E.** 1971. Cellular architecture of the *stratum corneum*. J Investig Dermatol **56:**165–169. http://dx.doi.org/10.1111/1523-1747.ep12260765.
23. **Bakaletz LO.** 2009. Chinchilla as a robust, reproducible and polymicrobial model of otitis media and its prevention. Expert Rev Vaccines **8:**1063–1082. http://dx.doi.org/10.1586/erv.09.63.
24. **Harrison A, Dyer DW, Gillaspy A, Ray WC, Mungur R, Carson MB, Zhong H, Gipson J, Gipson M, Johnson LS, Lewis L, Bakaletz LO, Munson RS, Jr.** 2005. Genomic sequence of an otitis media isolate of nontypeable *Haemophilus influenzae*: comparative study with *H. influenzae* serotype d, strain KW20. J Bacteriol **187:**4627–4636. http://dx.doi.org/10.1128/JB.187.13.4627-4636.2005.
25. **Goodman SD, Obergfell KP, Jurcisek JA, Novotny LA, Downey JS, Ayala EA, Tjokro N, Li B, Justice SS, Bakaletz LO.** 2011. Biofilms can be dispersed by focusing the immune system on a common family of bacterial nucleoid-associated proteins. Mucosal Immunol **4:**625–637. http://dx.doi.org/10.1038/mi.2011.27.
26. **Novotny LA, Jurcisek JA, Ward MO, Jr, Jordan ZB, Goodman SD, Bakaletz LO.** 2015. Antibodies against the majority subunit of type IV pili disperse nontypeable *Haemophilus influenzae* biofilms in a LuxS-dependent manner and confer therapeutic resolution of experimental otitis media. Mol Microbiol **96:**276–292. http://dx.doi.org/10.1111/mmi.12934.
27. **Novotny LA, Jurcisek JA, Godfroid F, Poolman JT, Denoel PA, Bakaletz LO.** 2006. Passive immunization with human anti-protein D antibodies induced by polysaccharide protein D conjugates protects chinchillas against otitis media after intranasal challenge with *Haemophilus influenzae*. Vaccine **24:**4804–4811. http://dx.doi.org/10.1016/j.vaccine.2006.03.021.
28. **Bakaletz LO, Kennedy BJ, Novotny LA, Duquesne G, Cohen J, Lobet Y.** 1999. Protection against development of otitis media induced by nontypeable *Haemophilus influenzae* by both active and passive immunization in a chinchilla model of virus-bacterium superinfection. Infect Immun **67:**2746–2762.
29. **Kennedy BJ, Novotny LA, Jurcisek JA, Lobet Y, Bakaletz LO.** 2000. Passive transfer of antiserum specific for immunogens derived from a nontypeable *Haemophilus influenzae* adhesin and lipoprotein D prevents otitis media after heterologous challenge. Infect Immun **68:**2756–2765. http://dx.doi.org/10.1128/IAI.68.5.2756-2765.2000.
30. **Sirakova T, Kolattukudy PE, Murwin D, Billy J, Leake E, Lim D, DeMaria T, Bakaletz L.** 1994. Role of fimbriae expressed by nontypeable *Haemophilus influenzae* in pathogenesis of and protection against otitis media and relatedness of the fimbrin subunit to outer membrane protein A. Infect Immun **62:**2002–2020.
31. **Brockson ME, Novotny LA, Jurcisek JA, McGillivary G, Bowers MR, Bakaletz LO.** 2012. Respiratory syncytial virus promotes *Moraxella catarrhalis*-induced ascending experimental otitis media. PLoS One **7:**e40088. http://dx.doi.org/10.1371/journal.pone.0040088.
32. **Jurcisek JA, Bookwalter JE, Baker BD, Fernandez S, Novotny LA, Munson RS, Jr, Bakaletz LO.** 2007. The PilA protein of non-typeable *Haemophilus influenzae* plays a role in biofilm formation, adherence to epithelial cells and colonization of the mammalian upper respiratory tract. Mol Microbiol **65:**1288–1299. http://dx.doi.org/10.1111/j.1365-2958.2007.05864.x.
33. **Armbruster CE, Hong W, Pang B, Weimer KE, Juneau RA, Turner J, Swords WE.** 2010. Indirect pathogenicity of *Haemophilus influenzae* and *Moraxella catarrhalis* in polymicrobial otitis media occurs via interspecies quorum signaling. mBio **1:**e00102–10. http://dx.doi.org/10.1128/mBio.00102-10.
34. **Szelestey BR, Heimlich DR, Raffel FK, Justice SS, Mason KM.** 2013. *Haemophilus* responses to nutritional immunity: epigenetic and morphological contribution to biofilm architecture, invasion, persistence and disease severity. PLoS Pathog **9:**e1003709. http://dx.doi.org/10.1371/journal.ppat.1003709.
35. **Mason KM, Munson RS, Jr, Bakaletz LO.** 2005. A mutation in the *sap* operon attenuates survival of nontypeable *Haemophilus influenzae* in a chinchilla model of otitis media. Infect Immun **73:**599–608. http://dx.doi.org/10.1128/IAI.73.1.599-608.2005.
36. **Johnson RW, McGillivary G, Denoel P, Poolman J, Bakaletz LO.** 2011. Abrogation of nontypeable *Haemophilus influenzae* protein D function reduces phosphorylcholine decoration, adherence to airway epithelial cells, and fitness in a chinchilla model of otitis media. Vaccine **29:**1211–1221. http://dx.doi.org/10.1016/j.vaccine.2010.12.003.
37. **Leroy M, Cabral H, Figueira M, Bouchet V, Huot H, Ram S, Pelton SI, Goldstein R.** 2007. Multiple consecutive lavage samplings reveal greater burden of disease and provide direct access to the nontypeable *Haemophilus influenzae* biofilm in experimental otitis media. Infect Immun **75:**4158–4172. http://dx.doi.org/10.1128/IAI.00318-07.
38. **Bouchet V, Hood DW, Li J, Brisson JR, Randle GA, Martin A, Li Z, Goldstein R, Schweda EK, Pelton SI, Richards JC, Moxon ER.** 2003. Host-derived sialic acid is incorporated into *Haemophilus influenzae* lipopolysaccharide and is a major virulence factor in experimental otitis media. Proc Natl Acad Sci U S A **100:**8898–8903. http://dx.doi.org/10.1073/pnas.1432026100.
39. **Ehrlich GD, Veeh R, Wang X, Costerton JW, Hayes JD, Hu FZ, Daigle BJ, Ehrlich MD, Post JC.** 2002. Mucosal biofilm formation on middle-ear mucosa in the chinchilla model of otitis media. JAMA **287:**1710–1715. http://dx.doi.org/10.1001/jama.287.13.1710.
40. **Giebink GS.** 1999. Otitis media: the chinchilla model. Microb Drug Resist **5:**57–72. http://dx.doi.org/10.1089/mdr.1999.5.57.
41. **Christophers E, Kligman AM.** 1964. Visualization of the cell layers of the *stratum corneum*. J Investig Dermatol **42:**407–409.
42. **Novotny LA, Partida-Sanchez S, Munson RS, Jr, Bakaletz LO.** 2008. Differential uptake and processing of a *Haemophilus influenzae* P5-derived immunogen by chinchilla dendritic cells. Infect Immun **76:**967–977. http://dx.doi.org/10.1128/IAI.01395-07.
43. **Murphy TF, Yi K.** 1997. Mechanisms of recurrent otitis media: importance of the immune response to bacterial surface antigens. Ann N Y Acad Sci **830:**353–360. http://dx.doi.org/10.1111/j.1749-6632.1997.tb51907.x.
44. **Holmgren J, Czerkinsky C.** 2005. Mucosal immunity and vaccines. Nat Med **11:**S45–S53. http://dx.doi.org/10.1038/nm1213.
45. **Wu HY, Russell MW.** 1997. Nasal lymphoid tissue, intranasal immunization, and compartmentalization of the common mucosal immune system. Immunol Res **16:**187–201. http://dx.doi.org/10.1007/BF02786362.